

Proteogenic Amino Acids: Chiral and Racemic Crystal Packings and Stabilities

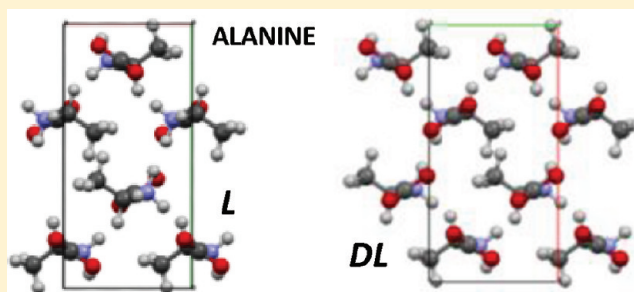
J. D. Dunitz*[†] and A. Gavezzotti*[§]

[†]Organic Chemistry Laboratory, HCI H333, ETH-Hönggerberg, Zurich, Switzerland

[§]Dipartimento di Chimica Strutturale e Stereochimica Inorganica, University of Milano, Milano, Italy

S Supporting Information

ABSTRACT: Crystal structures of chiral and racemic proteogenic amino acids are compared, over a database of 40 crystal structures and 20 chiral-racemic pairs. Wallach's rule does not apply. Solubility data show that the racemates tend to be slightly more stable than their chiral counterparts. Lattice energies are calculated by semiempirical PIXEL methods and by several ab initio methods, which also yield molecular energies. Results, especially molecular energies, are sensitive to small structural differences and therefore depend on the crystal structure accuracy. Surface effects in crystals of zwitterionic molecules require special attention. Energy differences between chiral and racemic crystals are typically around 10 kJ mol⁻¹, roughly the limit of our calculations. These suggest, however, that crystal stability tends to increase with decreasing crystal density, a result possibly related to the strong directionality of hydrogen bonds. The analysis of interaction energies between molecules related by specific symmetry operations shows that stabilization in homochiral crystal structures comes mainly from formation of screw-symmetric ribbons, whereas racemic crystal structures preferentially exhibit strongly stabilizing centrosymmetric dimers.



1. INTRODUCTION

The notion that racemic crystals are more tightly packed than their chiral counterparts, Wallach's rule, is more than a hundred years old.¹ Are they then more stable? one may ask. The packing argument rests on the assumption that in the periodic arrangement of a crystalline phase there are more ways to pack enantiomers than to pack molecules with the same chirality sense. All 230 space groups are available to racemates, including some of the most popular ones with organic compounds, such as *P*₂₁/*c* and *P*₁—which include symmetry operations of the second kind, namely glide planes and inversion centers, whereas homochiral crystals are restricted to the 65 space groups with only translation and proper rotation operations.

The definition of the two poles of the comparison, “racemic” and “chiral” structures, is not always clear-cut. Crystallization from homochiral solutions must lead to preservation of enantiomeric purity in the solid, but crystallization from a racemic solution offers a range of possibilities going from ordered racemates, to spontaneous resolution into a conglomerate, or to disordered or even twinned solids that may or may not contain equal amounts of the enantiomers. The rate of interconversion between enantiomers also plays a role in the crystallization process. Slowly interconverting enantiomers count as two phases, while rapidly interconverting enantiomers count as a single phase.² Differences in molecular structure among polymorphs are commonplace and result from conformational changes or from tautomerism. Besides, the relative stability of racemic and chiral

crystal forms, or that of different polymorphs, is temperature dependent.

There is also the question of what is meant by “more stable”. This could involve thermodynamic stability (lower free energy, $G = H - TS$), or merely more stabilizing lattice energy. In our work, only the latter is involved. Thus, we rely on results of computations at different levels of theory. For amino acids, we have atom–atom potentials at increasing level of sophistication, as pioneered by Scheraga and co-workers.^{3,4} We also have a choice among several top-level quantum chemical methods, as exemplified by ab initio studies on glycine⁵ and on layers of hydrophobic amino acids;⁶ and by ab initio calculations coupled to experimental charge density studies for alanine.⁷ The calculation of accurate crystal energies has recently led to conspicuous progress toward the de novo prediction of amino acid crystal structures.⁸

Following previous work along similar directions⁹ we here examine crystal and molecular structures of proteinogenic amino acids, which are invariably in zwitterionic form in the crystals. Molecular and crystal energies are evaluated for comparison of racemic and chiral pairs. For amino acid zwitterions, crystal stability depends on the packing requirements

Special Issue: Harold A. Scheraga Festschrift

Received: December 15, 2011

Revised: February 10, 2012

Published: February 23, 2012

beyond nearest neighbors and on the patterns of very strong hydrogen bonds, neither of which depend on density or on the close packing requirement typical of organic crystals where polarization-dispersion forces dominate. While some chiral and racemic pairs have closely related packings, other pairs exhibit unrelated packings based on different molecular conformations and hydrogen bonding patterns.

2. EXPERIMENTAL DATA

2.1. Crystal Structures. The availability of more than half a million crystal and molecular structure data from the Cambridge Structural Database (CSD),¹⁰ together with efficient methods for intermolecular energy calculations, provides a pathway for the analysis of crystal packing energies and geometries. The structural information from the CSD, derived by X-ray or neutron diffraction, consists of unit cell dimensions, space group and atomic coordinates for each crystal structure. This information can be used as basis for the calculation of lattice energies, which serve to assess the relative stability of the structures concerned, although with due caution. The atomic arrangements derived from diffraction analysis are subject to various types of uncertainty and error, some systematic, i.e., inherent in the interpretation of the experimental diffraction data, and others arising from faulty interpretation of the data. These uncertainties are reflected in the average standard uncertainties of atomic parameters (evaluated differently in different data processing softwares), in the anisotropic displacement parameters (ADPs), and in the final *R*-factor (an indicator of overall reliability but dependent to some extent on factors such as the choice of weighting schemes). Disorder in crystal structures is very common and thermal motion affects atomic positions, except for structures determined at temperatures close to 0 K. Thus, due caution is called for in the choice of crystal data and in the interpretation of the results of energy calculations.

- (a) Standard uncertainties of lattice parameters are usually vastly underestimated, and this is true to a large extent also of atomic positional and displacement parameters, because of inadequate weighting of the observational data, the scattering angles and intensities of diffracted beams, in least-squares calculations. Essentially, the observational data are treated as if they corresponded to the “correct” values of the observations, and no attempts are usually made to estimate their actual variances. As a consequence, small differences in experimental conditions may result in uncontrolled differences in the apparent molecular geometry, which, however small, affect the calculation of molecular energies.
- (b) As noted by Cruickshank more than sixty years ago,¹² rotational oscillations of rigid molecules or of atomic groups cause the apparent atomic positions, as estimated by diffraction methods, to be slightly displaced toward the rotation axis; that is, the molecules appear to shrink. Atomic separations computed from these positions cannot be interpreted directly as interatomic distances, a detail that is seldom considered in the estimation of lattice energies. Since X-rays are scattered by electrons, hydrogen atom positions determined by X-ray diffraction are not only imprecise but are also subject to systematic error; the redistribution of electron density on chemical bonding causes them to be apparently shifted from their actual nuclear sites toward the atoms to which they are bonded.

To correct this error, the hydrogen position can be moved along the X–H direction to increase the X–H distance to a standard value. Without such corrections, intramolecular X–H distances are too short and intermolecular distances involving hydrogen atoms in crystals are systematically too large. Errors arising from this source are especially serious in hydrogen bonded systems, where the hydrogen-bond energy is highly sensitive to the position of the hydrogen atom even when the O(N)⋯O(N) distance is accurately known. Neutron diffraction data are, of course, unaffected by this difficulty.

- (c) Multiple crystal structure analyses are often available for the same compound. In our work, CSD entries were selected by a balanced set of criteria: lower crystallographic *R*-factor, no disorder, neutron diffraction data when available, one entry for each crystal polymorph, same temperature for comparison of chiral-racemic pairs, as far as possible. Hydrogen atoms attached to carbon, oxygen or sulfur were relocated by the usual¹³ procedure (see Appendix 1, Supporting Information). Crystal densities *D* were renormalized to *D*⁰, the expected density at 295 K, as $D^0 = D \exp[\alpha(T - 295)]$, where $\alpha = (1/V) dV/dT$, the thermal expansion coefficient, was estimated as 10^{-4} K^{-1} from variable-*T* determinations of amino acid crystal structures.

2.2. Packing Analysis. Table 1 lists the amino acid crystal structures selected for our study. They are of heterogeneous source and accuracy. Some of the racemate structures are less reliable than those of the corresponding chiral crystals because they date from the early days of X-ray analysis and are thus based on visual examination of photographic diffraction patterns. Some amino acids are missing. These flaws and gaps in our knowledge of such important compounds should be correctable nowadays without too much trouble.

Since there are already innumerable accounts of the amino acid crystal structures, individual, collective, descriptive, classificatory, interpretative, we limit ourselves here to a few points that have emerged from the present survey and to some additional remarks that seem relevant to our new lattice energy calculations.

In the natural *S*-series, the smaller of the two N–C–C–O torsion angles always lies between 0 and -50° , thus tending to bring the $\text{C}\alpha\text{-C}\beta$ bond into an orientation that is more nearly perpendicular to the plane of the carboxylate group. Of the two carboxylate O atoms, one is thus syn with respect to the ammonium N atom, the other anti. One might expect that this difference would be associated with a difference in hydrogen bond acceptor ability, but there seems to be no obvious pattern. For those molecules where the NCCO torsion angle is close to zero (e.g., proline and serine) with a N⋯O distance of about 2.6 Å, one might be tempted to ascribe this feature to formation of an intramolecular hydrogen bond. In all cases, however, the N atom in question fulfils its quota of three (or two, for proline and histidine) intermolecular hydrogen bonds.

Quite often the racemic and chiral crystal structures are closely related with similar unit cell dimensions. Some even appear to be almost identical in projection down one of the crystal axes. Relative to the chiral structure, half the molecules in the racemate are viewed, so to say, in a mirror. In contrast, some racemic and chiral pairs are based on different molecular conformations, so that there is no such relationship between them. For example, in glutamic acid the conformation about the

Table 1. Selected Crystal Structures of Amino Acids.^a

compound	racemate				chiral			
	refcode	space group	R	T/K	refcode ^b	space group (Z') ^c	R	T/K
ala	DLALNI04	<i>Pna2</i> ₁	1.92	19	LALNIN24	<i>P2</i> ₁ <i>2</i> ₁ <i>2</i> ₁	1.59	23
					ALUCAL05(<i>D</i>)	<i>P2</i> ₁ <i>2</i> ₁ <i>2</i> ₁	7.9	60
arg	no data				no data			
asn	no data				VIKKEG	<i>P2</i> ₁	3.24	90
asp	DLASPA10	<i>C2/c</i>	3.1	RT	LASPR02	<i>P2</i> ₁	2.73	RT
cys	BOQCUF10	<i>P2</i> ₁ / <i>a</i>	7.1	100	LCYSTN04	<i>P2</i> ₁ (2)	3.11	120
					LCYSTN22	<i>P2</i> ₁ <i>2</i> ₁ <i>2</i> ₁	1.7	30
glut	YUYMOU	<i>P2</i> ₁ / <i>n</i>	3.8	RT	LGLUAC03	<i>P2</i> ₁ <i>2</i> ₁ <i>2</i> ₁ α	2.1	RT
					LGLUAC11	<i>P2</i> ₁ <i>2</i> ₁ <i>2</i> ₁ β	2.6	RT
gln	TACQUJ	<i>P2</i> ₁ / <i>c</i>	4.1	RT	GLUTAM01	<i>P2</i> ₁ <i>2</i> ₁ <i>2</i> ₁	3.2	RT
his	DLHIST01	<i>P2</i> ₁ / <i>c</i>	3.0	110	LHISTD04	<i>P2</i> ₁	3.9	RT
					LHISTD10	<i>P2</i> ₁ <i>2</i> ₁ <i>2</i> ₁	3.4	RT
ile	DLILEU02	<i>P</i> $\bar{1}$	5.8	150	LISLEU02	<i>P2</i> ₁ (2)	5.2	120
leu	DLLEUC	<i>P</i> $\bar{1}$	5.8	RT	LEUCIN02	<i>P2</i> ₁ (2)	4.4	120
					LEUCIN03	<i>C2</i>	3.3	RT
lys	no data				no data			
met	DLMETA05	<i>I2/a</i>	4.1	105	LMETON02	<i>P2</i> ₁ (2)	3.7	120
phe	no data				no data			
pro	QANRUT	<i>P2</i> ₁ / <i>c</i>	4.0	120	PROLIN	<i>P2</i> ₁ <i>2</i> ₁ <i>2</i> ₁	16.9	RT
ser	DLSEIN14	<i>P2</i> ₁ / <i>a</i>	2.3	100	LSEIN20	<i>P2</i> ₁ <i>2</i> ₁ <i>2</i> ₁	3.2	100
thr	no data				LTHREO02	<i>P2</i> ₁ <i>2</i> ₁ <i>2</i> ₁	6.8	RT
					LTHREO03	<i>P2</i> ₁ <i>2</i> ₁ <i>2</i> ₁	2.6	12
trp	QQQBTP02	<i>P2</i> ₁ / <i>c</i>	4.0	173	no data			
tyr	DLTYRS	<i>Pna2</i> ₁	3.7	RT	LTYROS11	<i>P2</i> ₁ <i>2</i> ₁ <i>2</i> ₁	4.0	RT
					FAZHET01(<i>D</i>)	<i>P2</i> ₁ <i>2</i> ₁ <i>2</i> ₁	3.1	91
val	VALIDL02	<i>P</i> $\bar{1}$	4.5	120	LVALIN01	<i>P2</i> ₁ (2)	3.4	120
					AHEJEC01(<i>D</i>)	<i>P2</i> ₁ (2)	3.2	173
gly			GLYCIN	<i>P2</i> ₁	3.2	RT		
			GLYCIN20	<i>P2</i> ₁ / <i>n</i>	2.7	RT		
			GLYCIN18	<i>P3</i> ₁	2.3	RT		

^aFor each entry: CSD refcode,¹⁰ space group, crystallographic *R*-factor, and temperature of data collection (RT = 285 ± 2 K). ^b*L* enantiomer unless otherwise specified. ^c*Z'*, number of molecules in the asymmetric unit, = 1 unless otherwise stated. Full crystallographic data are available as Table S1 in the Supporting Information.

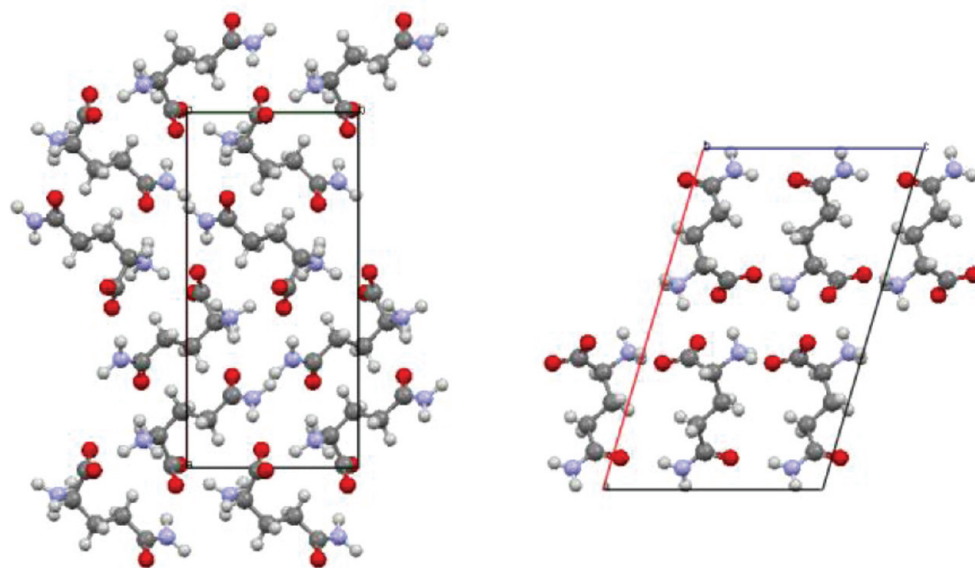


Figure 1. Crystal structures of L-glutamine (GLUTAM01, left) and D,L-glutamine (TACQUJ, right;) viewed in projection down their short cell axis. Remarkably, the racemate is 12% less dense than the chiral crystal. Figure drawn by Mercury.¹⁴

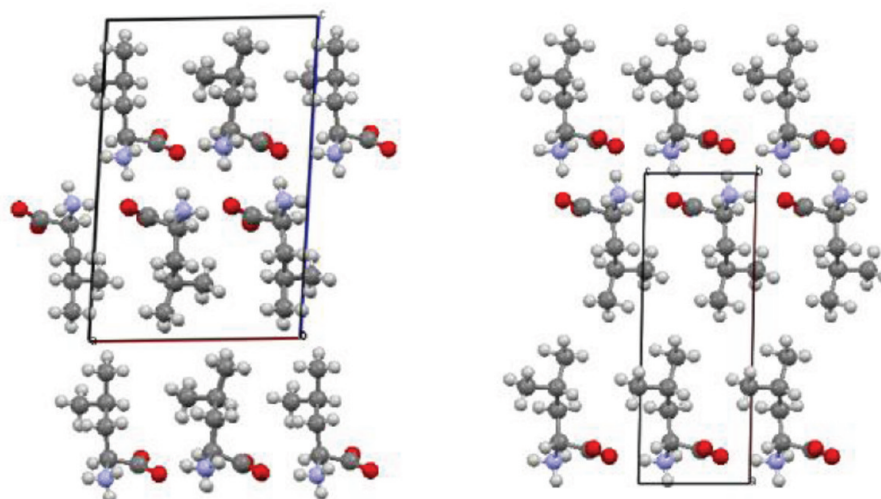


Figure 2. Crystal structure of L-leucine (LEUCIN02, left): molecules in horizontal rows are not symmetry related ($Z' = 2$), but mimic the true translational symmetry in the racemic crystal (DDLEUC, right; projection down the shortest axis (b) of each). Successive rows are related by 2_1 screw axes or by inversion symmetry, but arrangements are quite similar. This packing is typical for amino acids with aliphatic side-chains (Figure S1, Supporting Information). Figure drawn by Mercury.¹⁴

central C–C bond of the side chain is antiplanar in the racemate (torsion angle 175°) and gauche in the two chiral polymorphs ($+68$ and -73°): the packing in the three crystal structures is, of course, different.

Aspartic acid forms an intramolecular hydrogen bond only in the racemic crystal. Cysteine has two polymorphs for both racemic and chiral phases: the molecular conformations in the five symmetry independent molecules are different, especially the orientation of the C–S–H group (Table S2, Supporting Information), and the corresponding hydrogen-bonding patterns are different. The positions of hydrogen atoms bonded to a relatively strong scatterer like sulfur are subject to larger uncertainties than usual, and structural disorder at the thiol group is present at higher temperatures. Section 3 includes an analysis of how these similarities and differences affect our calculated energies.

The greatest difference in density in a L- D,L pair runs against expectation: the L-glutamine crystal is an astonishing 11.8% more dense than the racemate, a fact apparently neither noticed nor discussed up until now. The largest differences we had noted previously⁹ were of the order of 8% and were in the opposite direction. In D,L glutamine the side-chain is anti-planar to the ammonium group, in the chiral crystal it is gauche to both the ammonium and the carboxylate groups. In both crystal structures (Figure 1) each molecule is engaged in 10 hydrogen bonds, five N–H donor and five C=O acceptor, to 10 surrounding molecules in the chiral phase, but only to 9 in the racemate. Glutamic acid, with similar molecular weight, chemical structure, and hydrogen bonding possibilities, has a density close to that of L-glutamine (1.525 g cm^{-3}) in both chiral and racemate crystalline forms, so it is clearly D,L -glutamine (density 1.364 g cm^{-3}) that seems anomalous. This crystal has the double-layer structure typical of the amino acids with aliphatic side chains, additional hydrogen bonding at the carboxyl amide terminus, one N–H \cdots O bond between molecules in the same double layer, related by glide reflection, the other connecting molecules in adjacent double layers, related by inversion. The “void” analysis provided by the CCDC Mercury software¹⁴ shows that the racemic crystal structure indeed contains extensive empty regions between next-neighbor

molecules related by the c -axis translation of 9.93 \AA and linked via two glide-reflection operations. Each pair of glide related molecules is linked at both ends by N–H \cdots O hydrogen bonds, the near linearity of which tends to hold the aliphatic side-chains parallel and at a fixed distance. The restrictions arising from such a combination of strong, linear hydrogen bonds lead to a more open structure (one is reminded of the ice/liquid water density relationship). The chiral structure experiences no such restrictions and can therefore fill space more efficiently.

The two chiral crystal structures for histidine are closely related, the 9.47 \AA translation of the former being replaced by a screw axis in the latter ($c = 18.87 \text{ \AA}$). In both structures the ammonium group forms two intermolecular N–H \cdots O bonds and an intramolecular N–H \cdots N interaction with the *ortho*-N atom of the imidazole ring. The iminium N–H group is hydrogen bonded to a carboxylate O atom of the molecule separated by the c translation (or corresponding screw axis). In contrast, the racemic crystal has no intramolecular N–H \cdots N bond. Here the ammonium group forms two N–H \cdots O hydrogen bonds and one N–H \cdots N bond to the *ortho*-N of a different molecule, while the other imidazole N atom is involved in an N–H \cdots O interaction.

The two proline crystal structures show special features arising from the special features of the molecule itself, its ring structure, its iminium group, and its conformational rigidity. In both crystals the N–C–C–O grouping has syn-planar conformation, leading to intramolecular N \cdots O distances 2.60 – 2.65 \AA , short enough to be attributable to intramolecular hydrogen bonding. However, the NH_2^+ group is already engaged in two intermolecular hydrogen bonds to carboxylate groups. With only two, instead of the usual three intermolecular H bonds, proline is by far the most soluble of the proteogenic amino acids.

Serine adopts the same conformation in both the racemic and chiral crystals, with the hydroxyl group trans-planar to the α -H atom. The chiral crystal contains strings of O–H \cdots OH \cdots OH linkages along the a translation, whereas in the racemic crystal the hydroxyl group is hydrogen bonded to a carboxylate oxygen atom.

It is widely assumed¹⁵ that crystallization from a racemic solution of threonine leads to a conglomerate rather than to a

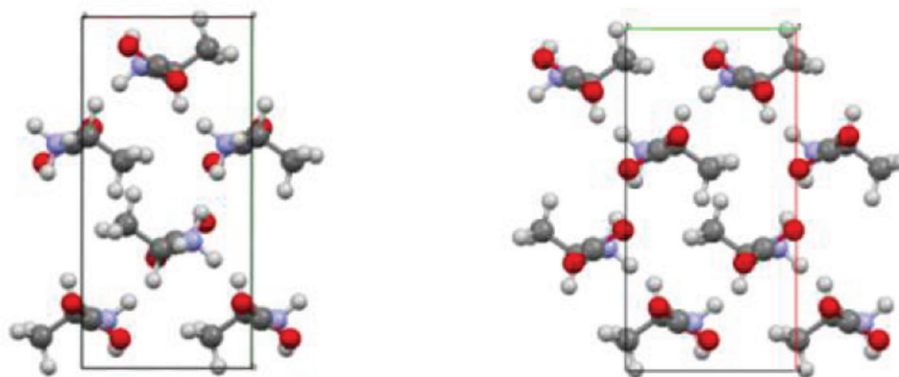


Figure 3. Crystal structures of *L*-alanine (LALNIN24, left) and *D,L*-alanine (DLALNI04, right) in projection along the *c* axis. Carboxylate groups point up and down in the *L* structure, and all up in the polar *D,L* structure. In the *L* structure alternate *yz* layers are related by screw axes, in the racemate by glide planes. Figure drawn by Mercury.¹⁴

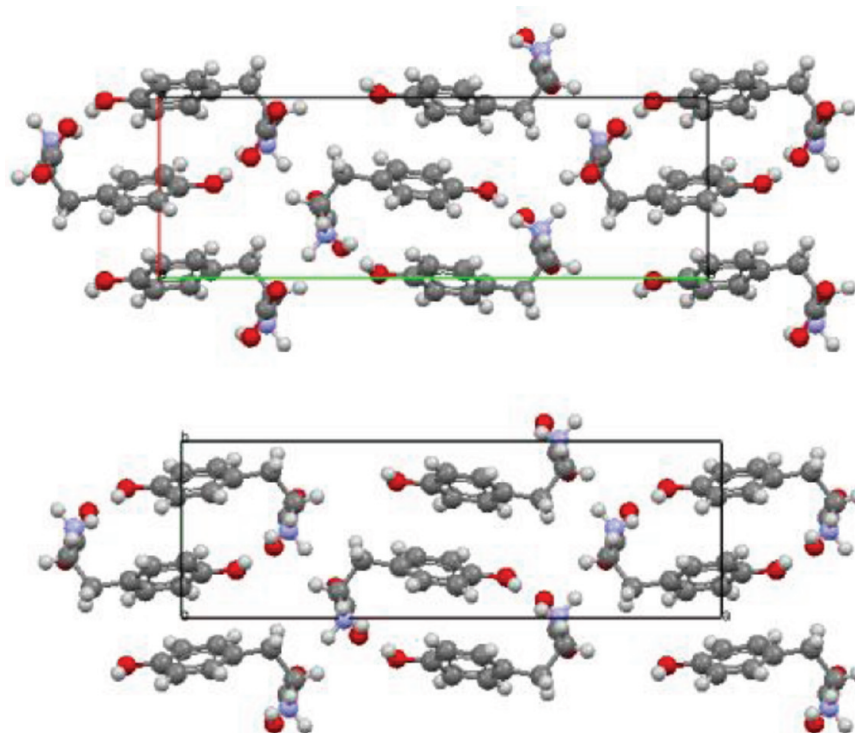


Figure 4. *L*-Tyrosine (LTYROS11, upper) and *D,L*-tyrosine (DLTYRS, lower) crystal structures, showing the similarity in projection down the *c* axis. As pointers of the difference, the hydroxyl H atoms all point upward in the polar chiral structure (screw axis), and point alternately up and down in the racemate structure (glide plane). Figure drawn by Mercury.¹⁴

racemate, but the evidence for this, although persuasive, is by no means conclusive. A preliminary crystallographic study¹⁶ found an orthorhombic unit cell with no systematic absences. From their external form, the crystals were described as belonging to the orthorhombic “hemihedral hemimorphic” class *mm* (C_{2v}) and were assigned the space group *Pmm*2. This assignment would impose impossible symmetry restrictions on the molecular packing and must be rejected. The subsequent determination of the crystal structure of *L*-threonine¹⁷ was a major achievement, as the most complex noncentrosymmetric organic crystal structure established by three-dimensional X-ray diffraction data at the time, it seems a pity that this structure does not appear in the CSD listings. Many years later, it was confirmed and refined by neutron diffraction (LTHREO02) and low-temperature (LTHREO03) studies). Shoemaker et al.¹⁷

found nearly the same cell dimensions as those reported earlier for the “racemate”¹⁶ and suggested that this material was actually a conglomerate of *D* and *L* crystals. We were not aware of any subsequent confirmation of the validity of this suggestion, which may be put in question by the fact that *L*- and *D,L*-alanine, and *L*- and *D,L*-tyrosine pairs have closely similar unit cell dimensions but do yield a racemate crystal. The formation of a conglomerate is now confirmed by a new study of the crystalline product from a racemic solution of threonine, in which all crystals examined had space group $P2_12_12_1$.¹⁸ It might be interesting to try to determine the conditions (temperature and pressure) under which the racemate might be obtainable.

Amino acids with weakly polar side chains (valine, leucine, isoleucine, methionine, cysteine and phenylalanine; see Table 1) form crystals with the double-layer structure discussed in

detail by several authors, especially by Gorbitz et al.⁶ The chiral crystals in space group $P2_1$ contain two symmetry-independent molecules related by a more or less close translation operation, in rough correspondence to the true translation operation in the $P1$ -racemate. Conformational differences are in some cases quite small, as for leucine (Figure 2), and in other cases so large that the two independent molecules are in fact conformational isomers. A general feature of all these structures is that two N–H...O hydrogen bonds form characteristic layers, and the third holds a pair of antipolar layers together to form a double layer. The periodicity in this direction depends on the length of the side-chain, while the periodicities within the layers do not vary much within the series. The general similarity between chiral and racemic structures of this group is best seen in projection down the short axis (Figure 2). Separate layers in the double layers are related by screw axes in the chiral structure, and by inversion centers in the racemate.

In both racemic and chiral alanine crystals, H-bonded chains run parallel to the three crystal translations. The unit cell translations are almost identical. Indeed, the two structures viewed in projection down their respective c axes (Figure 3) appear to be almost identical. In the chiral structure neighboring chains running along the screw axes parallel to c are homochiral but run in opposite directions, whereas in the racemate structure neighboring chains are of opposite chirality but run in the same direction, being related by glide reflection symmetry. This generates a large net polarity that makes D,L-alanine an ideal system for experiments on control of crystal growth by tailor-made impurities.¹⁹

The crystal structures of L- and D,L-tyrosine are also closely related, as pointed out many years ago.²⁰ The molecular conformation is almost the same and unit cell dimensions are closely similar. The space groups are related in the same way as for L- and D,L-alanine (Table 1; see also Figure S2, Supporting Information). Figure 4 shows the two structures in projection down the c axis, the polar axis of the racemate. All hydroxyl H-atoms point downward in the racemate, while in the chiral structure they point in opposite directions in alternating layers, which are related by screw axes in the chiral structure and by glide planes in the racemate.

2.3. Solubility Data. For organic compounds, the usual method of confronting calculated lattice energies with experiment is by comparison with sublimation enthalpies.²¹ Amino acids, however, have zwitterionic structures with relatively high melting temperatures, and tend to decompose on heating. The transition to the gas-phase species is invariably associated with large charge reorganization and a correspondingly large energy change. Experimental sublimation enthalpies for these compounds are difficult to measure, and, when available, are often denoted as “unreliable”.²² As an alternative, for racemic and chiral crystal pairs the difference in lattice energy should be close to the difference in solution enthalpy, because the interactions of the solute molecules with an achiral solvent should be the same for both enantiomers. Measurements of amino acid solubility in water (Table 2) are available for six pairs of L and D,L pairs from early work²³ carried out with exemplary care and attention, although, almost eighty years later, one may be concerned with the purity of the amino acid samples obtained before chromatographic methods came into use. Besides, it is not always clear whether the racemic material was a true racemate or a conglomerate or a mixture of these. Furthermore, many of the compounds used in the solubility experiments show polymorphism, and we do not know which

Table 2. Enthalpies and Entropies of Solution of Amino Acid Crystals^a

	R^{2b}	$\Delta H(\text{soln})$ kJ mol ⁻¹	$\Delta S(\text{soln})$ J mol ⁻¹ K ⁻¹	$\Delta\Delta H(\text{chiral-racemate})^c$
L-ala	0.996	8.65	71.7	
DL-ala	0.996	10.39	77.5	-1.74
L-asg	1.00	28.13	108.1	
DL-asg	1.00	30.15	118.3	-2.02
L-glu	1.00	29.88	118.5	
DL-glu	1.00	28.22	120.1	1.66
L-leu	0.92	5.87	46.4	
DL-leu	0.97	11.72	58.7	-5.85
L-tyr	1.00	25.09	77.8	
DL-tyr	1.00	25.94	78.6	-0.85
L-phe	0.99	13.60	74.1	
DL-phe	0.96	16.20	76.9	-2.60

^aEstimated by the van't Hoff equation from literature²³ solubility measurements. ^bReliability parameter for the linear fit. ^c $\Delta\Delta H = \Delta H(\text{soln, chiral}) - \Delta H(\text{soln, racemate})$.

polymorph was used. Anyway, in all cases the van't Hoff plots are consistently linear (Figure S3, Supporting Information) and yield enthalpies and entropies of solution shown in Table 2. For all six pairs $\Delta S(\text{soln})$ is slightly larger for the racemate, as expected, and with one exception (glutamic acid) $\Delta H(\text{soln})$ is also slightly larger, i.e., the racemates are slightly more stable than the chiral crystals. The same conclusion was reached²⁴ on the basis of calorimetric measurements of heats of solution of several proteogenic and other amino acid pairs. However, as in Table 2, energy differences are all within 6 kJ mol⁻¹, an amount that challenges the present limit of accuracy in any kind of theoretical calculation.

3. COMPUTATIONAL METHODS AND RESULTS

3.1. Intermolecular Energies. Lattice energies and molecular pair interaction were calculated by PIXEL, apportioned in their Coulombic, polarization, dispersion and repulsion terms^{25,26} (see Appendix 2, Supporting Information). Molecular electron densities were calculated by Gaussian²⁷ at the MP2/6-31G** level. The model crystal is represented by a cluster of molecules generated from a reference molecule, according to space-group symmetry. Molecules in the cluster are all those within a given cutoff distance between molecular centers of mass.

The lattice summations for the Coulombic energy of a crystal converge slowly because of the R^{-1} dependence on distance. When zwitterions are arranged with a large dipole moment component along a polar crystal direction, there is an additional problem. The crystal surfaces perpendicular to this direction contribute to the lattice energy with a strong anisotropic factor which is not adequately represented by the usual lattice sums based on interactions with a given central molecule. The problem has been dealt with²⁸ using reciprocal space methods that require an empirical adjustable parameter, not always transferable. As shown by van Eijck and Kroon,²⁹ an equivalent correction can be more readily obtained in a real-space approach:

$$E_{\text{Coul}} = U_1 + E(\text{surface}) = U_1 - 2\pi D_c / (3NV_c) \quad (1)$$

where U_1 is the lattice sum carried out to a large cutoff, D_c is the magnitude of the total cell dipole moment, and N is the number of molecules in the unit cell of volume V_c .

Polarization energies suffer from the same problem, although to a lesser extent because of the approximately R^{-3} dependence

on distances. An empirical correlation between the PIXEL Coulombic and polarization energies has been derived

$$E_{\text{pol}}(\text{kJ mol}^{-1}) = 0.440E_{\text{Coul}} + 18.75 \quad (2)$$

In this work, the PIXEL Coulombic energy was calculated at a cutoff of 30 Å and corrected by eq 1 for polar crystal structures with strong, aligned dipoles (about 15% of the occurrences). For uniformity, polarization energies were re-estimated according to eq 2. For nonzwitterionic organic compounds the above corrections are negligible except in a very few special cases.²⁶ Crystal model construction, energy convergence details, together with more complete validation of eqs 1 and 2 are described in Appendix 3, Supporting Information.

The reliability of the PIXEL method for the calculation of intermolecular energies of zwitterions has been confirmed by comparisons with ab initio calculations on glycine dimers (Figure S4 and Table S3, Supporting Information). Table 3

Table 3. Coulombic and Total Lattice Energy of Crystals of L- and D,L-Alanine

	LALNIN24 ^a	DLALNI04 ^a
PIXEL E_{coul}	−270.0	−113.3
PIXEL $E(\text{surface})$		−161.4
PIXEL $E_{\text{coul}} + E(\text{surface})$	−270.0	−274.7
PIXEL E_{tot}	−257.4	−72.6
PIXEL $E_{\text{tot}} + E(\text{surface})$	−257.4	−234.0
PIXEL Coulomb- and polarization-corrected	−267.9	−275.1
B3LYP E_{tot} ^a	−216	−215
B3LYP/D E_{tot} ^b	−269	−272
exptl. lattice energy ^{a,c}	275, 277	

^aReference 7. ^bReference 30. ^cReference 3 and references therein. kJ mol^{−1} units.

provides comparisons of PIXEL with periodic-orbital ab initio calculations³⁰ for L- and D,L-alanine with its highly polar structure. The uncorrected PIXEL Coulombic energy for the latter is much too small compared with the result for the chiral structure but is brought into line by the $E(\text{surface})$ correction. Note also that the agreement between surface corrected PIXEL and dispersion-corrected DFT (B3LYP/D) is excellent, while uncorrected B3LYP is way off the mark.

3.2. Molecular Energies. Molecular energies E_{mol} were calculated by MP2/6-31G** on the basis of molecular models extracted directly from the crystal structures, i.e., without energy minimization. They are orders of magnitude larger than lattice energies, but it is only the energy differences associated with differences in molecular geometry, and, especially with differences in the estimated H-atom positions, that are of interest to us here. We define the molecular energy difference as $\Delta E_{\text{mol}} < 0$ when the molecule extracted from the racemate crystal is more stable than that from the chiral crystal. Our experience with duplicate crystal structures shows, not surprisingly, that higher *R*-factor goes with higher molecular energy, calling for caution in the interpretation of such results, as small errors in bond distance or bond angle can result in a large ΔE_{mol} . As an example, the published structure of the high-temperature polymorph of D,L-cysteine (BOQCUF) shows an atypical C–S–H angle of 120°; setting this angle to 109° stabilizes the molecule by 27 kJ mol^{−1}.

The relative stability of crystals should be judged by comparison of the sum of the molecular energy difference ΔE_{mol} and the lattice energy difference ΔE_{latt} . As result of

approximations inherent to the methods described in the above sections, an energy difference less than about 10 kJ mol^{−1} falls within the uncertainty level of the calculations, but a difference in excess of 20 kJ mol^{−1} is surely significant. Lists of all compounds and crystal structures considered here with molecular and intermolecular energies are available in Table S4 of Supporting Information.

3.3. Crystal Coordination Modes. To analyze crystal packing, we consider the symmetry relationship and the interaction energy between a “reference” molecule and each of its surrounding ones (full detail is in Appendix 4, Supporting Information). Figure 5 shows the results for the chiral crystals.

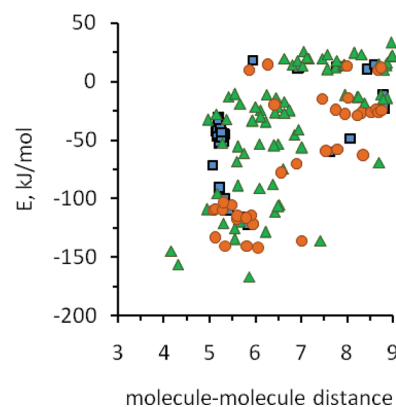


Figure 5. Molecule–molecule interaction energies as a function of distance between centers of mass for chiral amino acid crystals. Squares, translation; triangles, screw; circles, asymmetric. Screw-axis related and asymmetric partners are the most cohesive ones.

In the first coordination shell there are strongly stabilizing screw-axis relationships, and/or asymmetric couplings in $Z' = 2$ crystals (Table 1), with cohesion energies 90–170 kJ mol^{−1}. Figure 6 shows the corresponding picture for the racemates,

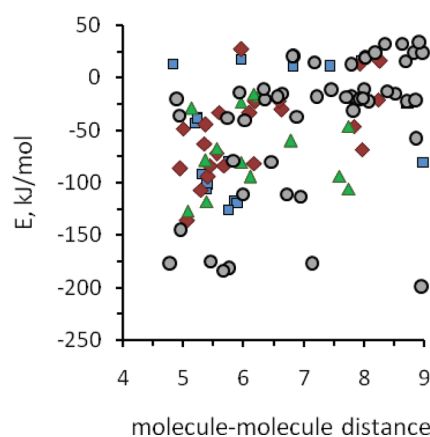


Figure 6. As in Figure 5, for racemic amino acid crystals. Squares, translation; diamonds, glide; triangles, screw; circles, inversion. Inversion-related partners are the most cohesive ones.

with strongly stabilizing centrosymmetric coupling and cohesion energies of 100–200 kJ mol^{−1}. Partners related by pure translation also make a substantial stabilizing contribution (30–120 kJ mol^{−1}) in both chiral and racemic crystals. Notably, some short-range and many long-range interactions are significantly repulsive. This is a consequence of the zwitterionic nature of the amino acid molecules in the crystals, as in ionic

Table 4. Densities and Calculated Energies of Amino Acids (kJ mol^{-1} units) for 40 Crystals and 20 Racemic-Resolved Crystal Pairs.^a

pair no.	CSD refcode	density ^b		$E(\text{lattice})^c$		$\Delta E(\text{mol})^d$	$\Delta E(\text{mol}) + \Delta E(\text{lattice})^d$
	racemic chiral	rac.	chir.	rac.	chir.		
1 pro	QANRUT-PROLIN	1.385	1.412	-198	-188 ^e	-13.0	-22.5
2 ile	DLILEU02-LISLEU02	1.237	1.203	-245	-257	-0.5	11.3
3 val	VALIDL02-LVALIN01	1.331	1.262	-251	-264	-3.4	10.5
4	VALIDL02-AHEJEC01	1.331	1.270	-251	-271	-5.6	14.5
thr	-LTHREO02		1.450	-257			
	-LTHREO03		1.449	-255			
5 leu	DLLEUC-LEUCIN02	1.191	1.166	-262	-264	1.5	3.3
6	DLLEUC-LEUCIN03	1.191	1.173	-262	-251	4.0	-7.5
7 asp	DLASPA10-LASPT02	1.644	1.643	-265	-288	-40.2	-16.7
8 ala	DLALNI04-LALNIN24	1.389	1.367	-275	-268	-0.5	-7.8
9	DLALNI04-ALUCAL05	1.389	1.371	-275	-275	-1.0	-0.9
10 ser	DLSERN14-LSERIN20	1.512	1.544	-289	-307 ^e	1.6	19.6
11 met	DLMETA05-LMETON02	1.341	1.350	-289	-274	4.7	-10.0
12 cys	BOQCUF10- LCYSTN22	1.478	1.489	-293	-259	24.4	-9.9
13	BOQCUF10- LCYSTN04	1.478	1.497	-293	-288	-10.4	-15.4
14 glu	YUYMOU-LGLUAC03	1.593	1.532	-303	-323	-17.8	2.4
15	YUYMOU-LGLUAC11	1.593	1.576	-303	-318	-20.9	-6.5
trp	QQQBTP02 -		1.354	-307			
16 tyr	DLTYRS-LTYROS11	1.436	1.414	-308	-305	9.0	5.4
17	DLTYRS-FAZHET01	1.436	1.404	-308	-302	2.9	-3.4
asn	- VIKKEG		1.574	-318			
18 gln	TACQUJ-GLUTAM01	1.364	1.525	-323	-321	1.8	-0.3
19 his	DLHIST01-LHISTD10	1.522	1.441	-337	-277	57.7	-2.4
20	DLHIST01-LHISTD04	1.522	1.442	-337	-282	52.5	-2.6
gly	GLYCIN β	1.584		-263		0	0
	GLYCIN20 α	1.614		-261		-1 ^e	+1 ^e
	GLYCIN15 γ	1.584		-257		-6 ^e	0 ^e

^aDifferences in Coulombic and dispersion lattice energies are listed in Table S7, Supporting Information. Energy differences below 10 kJ mol^{-1} may be at the limit of computational accuracy. ^bDensities (g cm^{-3}) are temperature-normalized (see text section 2.1) and are given to three decimal places in keeping with typical standard uncertainties in unit cell volume.³⁵ ^cPIXEL lattice energies (see text section 3.1). ^dDifference in molecular energy; $\Delta E's < 0$ if racemic is more stable. ^eRelative to the most stable polymorph. In italics, results based on inaccurate X-ray diffraction data.

crystals such as NaCl. The total interaction energy of nearest-neighbor partners is roughly equal to the Coulombic contribution, not because the other contributions are small, but because they cancel out almost exactly (Figure S5, Supporting Information). This explains the partial success of uncorrected DFT methods in such cases.

The racemates fall into three classes (Table S5, Supporting Information): (a) crystals (leu, val, his, glu, trp, and pro) where the most stabilizing partner is a centrosymmetric dimer linked by ammonium-carboxylate hydrogen bonds, and where there is a clear relationship between $\text{H}\cdots\text{O}$ distance and dimer energy; (b) crystals (asp, ser, lys, met, and gln) where the main hydrogen bond links molecules along a screw ribbon, with a more or less constant intermolecular separation of 5.5 \AA ; (c) two crystals, ala and tyr, in space group $Pna2_1$, where glide related hydrogen-bond ribbons of periodicity 6 \AA run along the polar c axis, with a substantial contribution from surface energy. There is no obvious dependence on the size and nature of the side chain.

The chiral crystals fall into two classes (Table S6, Supporting Information): (a) crystals (ser, ala, tyr, gln, glu, asn, asp, thr, his, and pro) forming screw ribbons in space group $P2_12_12_1$ with intermolecular distance from 5 to 7.5 \AA and constant hydrogen bonding geometry (with the exception of pro); (b) crystals (val, leu, ile, met, and cys) containing symmetry independent A–B pairs in space group $P2_1$, $Z' = 2$, having in common an

aliphatic side chain. In these crystals, an A–B pair is invariably the most cohesive one, with roughly constant energy irrespective of the side chain. Although these crystals have a polar space group, the A–B pairs are arranged (Figure 2a) so that the net dipole along the polar axis is very small and the surface energy is negligible. For the same reason the surface energy is almost zero in LEUCIN03, space group $C2$ with a cyclic dimer over a 2-fold axis.

3.4. Energy and Density Differences between Chiral and Racemic Crystal Pairs. Calculated lattice energies (Table 4) range from about 200 to about 330 kJ mol^{-1} , depending on hydrogen bonding ability but not primarily on molecular size. The energy for the smallest amino acid, glycine, is not the smallest in the list: that place is taken by proline, with only two intermolecular hydrogen bonds per molecule. The crystals with the largest lattice energies are glu and L-asn, with five intermolecular hydrogen bonds per molecule, and D,L-his, with four. Calculated energy differences between chiral and racemic amino acid crystal pairs are small (Table 4), either because $\Delta E(\text{lattice})$ and $\Delta E(\text{mol})$ are both small, or, more interestingly, because they have opposite signs. Where the molecular conformations differ (asp, cys, glu, and his), there is a kind of balance between conformational and lattice energy differences. Out of the twenty pairs appearing in Table 4, $\Delta E(\text{total})$ exceeds our significance limit of 10 kJ mol^{-1} in only six cases, and by a large amount only in two cases. Both are

questionable. One is proline, where the *R*-factor of the structure with the high energy molecule is as large as 16% and the suspicion of inaccuracies in molecular geometry is surely justified. The other, serine, is an outlier in the polarization energy correlation plot of eq 2, leading to an abnormally high $\Delta E(\text{lattice})$. Unfortunately, apart from the limited solubility data (Table 2), which confirm that energy differences between racemic and chiral crystal pairs are small, we have no reliable experimental data for comparison with the calculated energy differences.

Even for glutamine, in spite of the 12% density difference between the racemic and chiral crystals, the calculated lattice energies are nearly equal. The PIXEL decomposition (Table S8, Supporting Information) shows that the racemate is more strongly hydrogen-bonded (Coulombic/polarization), while the chiral crystal has better dispersive interactions. The density of the racemate is lower because of the strongly directional hydrogen bonds, which lead to a more open structure, as described in section 2.2.

The racemic partner is more dense in 70% of the cases, hardly the basis for a rule. Figure 7 shows that, with the

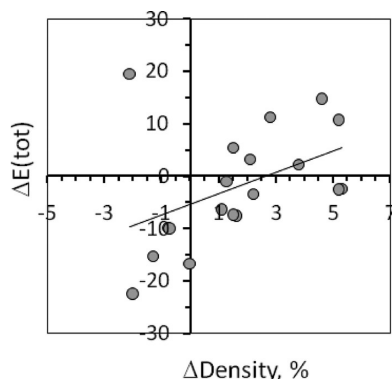


Figure 7. Racemic and chiral crystal pairs: total energy difference (<0 if racemic is more stable) as a function of density difference (>0 if racemic is more dense). With the exception of glutamine ($\Delta\text{Density} = -12\%$, not shown) there is a clear trend to more stability with lower density.

exception of glutamine and serine (see above), there is a clear trend to more stabilizing total energy with decreasing density. The analogy with the structure of ice comes to mind. There is, however, a significant correlation between higher density and more stabilizing dispersion energy, and a weaker correlation between higher density and lower Coulombic-polarization energies (Figure S6, Supporting Information).

The last three lines of Table 4 show a comparison among the polymorphs of glycine, which crystallizes in chiral (β and γ) and achiral (α) polymorphs. Differences here are so small as to prevent a reliable conclusion on relative stabilities.

4. DISCUSSION AND CONCLUSIONS

As an indication of the reliability of our computational procedures, for zwitterion dimers we have almost perfect coincidence between the PIXEL and the MP2/631G** potential energy curves for glycine. The good performance of the PIXEL formalism for the calculation of lattice energies has been established over the years and confirmed by detailed comparisons with high quality ab initio results (see ref 30 and references therein). In the crystal database for the present work,

30% of the entries are in space groups with polar axes. In such cases, Coulombic energies must be corrected by the surface energy method²⁹ as proposed earlier³⁰ and further validated here even for the strong zwitterionic dipoles (although the correction is significant only for about half the cases). A similar but empirical correction is necessary also for polarization energies. For glycine, with polymorphs in polar and nonpolar space groups, a high quality ab initio study³¹ has yielded lattice energy differences relative to the β polymorph as $\alpha = +1 \text{ kJ mol}^{-1}$, $\gamma = +5 \text{ kJ mol}^{-1}$, in perfect although perhaps fortuitous agreement with results shown in Table 4, these differences being close to computational accuracy level.

Our results also agree qualitatively with an HF-LCAO calculation on crystals of hydrophobic amino acids, where two classes of hydrogen bonding patterns show an energy difference of $15\text{--}20 \text{ kJ mol}^{-1}$,³² our energy difference is $\sim 30 \text{ kJ mol}^{-1}$, in the same direction but larger, as expected, due to the lack of dispersion contributions in the HF calculation. On the basis of present and past experience, our calculated lattice energies are more reliable than those of uncorrected DFT, and probably about as reliable as those of dispersion-corrected DFT.³³ The data in Table 4 stand as a challenge to future lattice energy calculations by quantum chemical methods.

Molecular energies (energies of formation from separate atoms) have been evaluated at the MP2/631G** level. In a few cases, where conformational energy differences are significant or where intramolecular and intermolecular hydrogen bonding are in competition, the MP2 difference in molecular energy very nearly balances the PIXEL difference in lattice energy, thus providing a clear picture of the interplay between intra- and intermolecular energy in crystals. We find, however, that minor structural differences arising from different X-ray determinations may be amplified into large molecular energy differences without real justification. In fact, ab initio molecular and lattice energy optimization is now being routinely used to validate experimental crystal structures of organic materials.³⁴

For amino acids, Wallach's Rule¹ does not apply. Racemates are not systematically more dense than their chiral counterparts and, indeed, the largest density difference, that for glutamine, an astonishing 12%, runs in the opposite direction (Figure 1). However, limited solubility data do show a tendency for racemates to be thermodynamically more stable (Table 2), but only by a small amount, less than 6 kJ mol^{-1} . In any case, the general rule often assumed for polymorphs, the denser, the more stable, does not seem to apply here. Although such small energy differences lie within the reliability limit of our calculations, some trends may be discerned: the less dense partner tends indeed to have the more stabilizing energy (Figure 7). It seems unlikely that random or systematic errors have converged to create this correlation.

The unifying motif in all amino acid crystal packings is, of course, $\text{NH}_3^+\cdots\text{OOC}$ hydrogen bonding, leading to a few characteristic patterns. For the racemates, centrosymmetric dimers dominate, but in D,L-alanine and D,L-tyrosine (Figures 4 and 5) polar chains related by glide plane symmetry run along a polar crystal axis. In chiral crystals, screw or translation ribbons dominate. In those with aliphatic side-chains, symmetry independent molecules form quasi-centrosymmetric dimers (Figure 2), and there is a single example of a homochiral cyclic dimer. Side chains adapt to these patterns by conformational flexibility. We find that $\text{N-H}\cdots\text{O}$ hydrogen bonds along a chain tend to be shorter than corresponding bonds in centrosymmetric dimers (average 1.82 against 1.92 \AA , all distances with

renormalized N–H distances), and that the cohesion energy of the dimer is always about 15% less than twice the energy of a single H-bond along a chain (Tables S5 and S6, Supporting Information). The preference for centrosymmetric pairing in racemates and for infinite chains in homochiral amino acids may persist in solution and may point toward a greater tendency toward polymerization in the chiral chains. This may hint at possible scenarios for the emergence of biochirality, but we prefer to leave discussion of this point to others.

Our present study lacks a discussion of the role of temperature and pressure. Our calculated energies are based on atomic coordinates determined by X-ray or neutron diffraction at some definite temperature. Where multiple determinations at different temperatures are available (e.g., D,L-cysteine, Figure S7, Supporting Information) total energy differences are less than 5 kJ mol⁻¹ over ranges of 200 K, and are thus barely significant. Exclusion of temperature also neglects entropic contributions to the free energy. In principle, these can be estimated from knowledge about lattice vibrations, but this information must rely today on approximate atom–atom force-field calculations or on ab initio methods too expensive for massive application to our database.

The present study has been hampered more by lack of experimental data than by shortcomings in computational resources. For example, while the Cambridge Database has no less than 66 different crystal structure determinations for glycine, crystal structures of some amino acids are still missing and others were determined in bygone times with lower accuracy than is now available. We must also make do with incomplete solubility and thermodynamic data. A relatively modest and inexpensive research program should be able to fill these gaps, but in the present academic milieu a program for amino acid purification, recrystallization, thermal analysis, X-ray diffraction and solubility measurements is unlikely to meet a favorable reception from funding agencies. Even if such modest funding were obtainable, it will not be easy to find a young scientist willing to undertake such outmoded, unspectacular, and, let us face it, possibly boring work, leading only to publications in low impact index journals. An alternative might be to share out the work as part of undergraduate laboratory programs at several universities over the world, but an organization to distribute the work and collate the results is so far nonexistent. We are not optimistic that the missing information will be provided as prerequisite for further confrontation of theoretical and experimental work on the proteogenic amino acids, but we hope we are mistaken.

■ ASSOCIATED CONTENT

■ Supporting Information

Appendices 1–4. Tables S1–S8 and Figures S1–S7. This material is available free of charge via the Internet at <http://pubs.acs.org>.

■ AUTHOR INFORMATION

Notes

The authors declare no competing financial interest.

■ NOTE ADDED IN PROOF

The crystal structure of L-arginine has now been published: Courvoisier, E.; Williams, P. A.; Lim, G. K.; Hughes, C. E.; Harris, K. D. M. *Chem. Comm.* **2012**, 48, 2761–2763.

■ ACKNOWLEDGMENTS

We are most grateful to Prof. Dieter Seebach for providing us with material crystallized from a racemic solution of threonine and to Dr. Bernd Schweizer for performing X-ray analysis and informing us that this material is a conglomerate. Periodic orbital calculations for alanine were carried out by CRYSTAL09.³⁶ This work has been made possible through facilities provided by the Cambridge Crystallographic Data Centre.

■ REFERENCES

- (1) Wallach, O. *Liebigs Ann. Chem.* **1895**, 286, 90–143.
- (2) For an achiral molecule crystallizing in a chiral space group, e.g., glycine, the Gibbs phase rule requires that the two enantiomorphic types of crystal count as a single phase. Otherwise, for the system consisting of solid, liquid and vapor in equilibrium, the relation $F = C + 2 - P$ would lead to -1 degrees of freedom for the system.
- (3) Momany, F. A.; Carruthers, L. M.; Scheraga, H. A. *J. Phys. Chem.* **1974**, 78, 1621–1630.
- (4) Kwon, O. Y.; Kim, S. Y.; No, K. T.; Kang, Y. K.; Jhon, M. S.; Scheraga, H. A. *J. Phys. Chem.* **1996**, 100, 17670–17677.
- (5) Volkov, A.; King, H. F.; Coppens, P. *J. Chem. Theor. Comp.* **2006**, 2, 81–89.
- (6) Gorbitz, C. H.; Vestli, K.; Orlando, R. *Acta Crystallogr.* **2009**, B65, 393–400.
- (7) Destro, R.; Soave, R.; Barzaghi, M. *J. Phys. Chem.* **2008**, B112, 5163–5174.
- (8) Gorbitz, C. H.; Dalhus, B.; Day, G. M. *Phys. Chem. Chem. Phys.* **2010**, 12, 8466–8477.
- (9) Brock, C. P.; Schweizer, W. B.; Dunitz, J. D. *J. Am. Chem. Soc.* **1991**, 113, 9811–9820.
- (10) Allen, F. H. *Acta Crystallogr.* **2002**, B58, 380–388.
- (11) Dunitz, J. D.; Schomaker, V.; Trueblood, K. N. *J. Phys. Chem.* **1988**, 92, 856–867.
- (12) Cruickshank, D. W. D. *Acta Crystallogr.* **1956**, 9, 757–758.
- (13) Gavezzotti, A. *CrystEngComm* **2008**, 10, 389–398.
- (14) Macrae, C. F.; Bruno, I. J.; Chisholm, J. A.; Edgington, P. R.; McCabe, P.; Pidcock, E.; Rodriguez-Monge, L.; Taylor, R.; van de Streek, J.; Wood, P. A. *J. Appl. Crystallogr.* **2008**, 41, 466–470.
- (15) Klusmann, M.; Iwamura, H.; Mathew, S. P.; Wells, D. H.; Pandya, U.; Armstrong, A.; Blackmond, D. G. *Nat. Chem.* **2006**, 441, 621–623.
- (16) Albrecht, G.; Schnakenberg, G. W.; Dunn, M. S.; McCullough, J. D. *J. Phys. Chem.* **1943**, 47, 24–30.
- (17) Shoemaker, D. P.; Donohue, J.; Schomaker, V.; Corey, R. B. *J. Am. Chem. Soc.* **1950**, 72, 2328–2349.
- (18) Schweizer, B. W. Personal communication.
- (19) Weissbuch, I.; Lahav, M.; Leiserowitz, L. *Cryst. Growth Des.* **2003**, 3, 125–150.
- (20) Mostad, A.; Nissen, H. M.; Romming, C. *Acta Chem. Scand.* **1972**, 26, 3819.
- (21) Gavezzotti, A. *Molecular Aggregation*; Oxford University Press: Oxford, U.K., 2007; Chapter 8.
- (22) Chickos, J. S. Heat of Sublimation Data. In *NIST Chemistry WebBook, NIST Standard Reference Database Number 69*; Linstrom, P. J., Mallard, W. G., Ed.; National Institute of Standards and Technology: Gaithersburg, MD, 2003; <http://webbook.nist.gov>.
- (23) Dalton, J. B.; Schmidt, C. L. A. *J. Biol. Chem.* **1933**, 103, 549–578.
- (24) Matsumoto, M.; Amaya, K. *Bull. Chem. Soc. Jpn.* **1980**, 53, 3510–3512.
- (25) Gavezzotti, A. *Mol. Phys.* **2008**, 106, 1473–1485.
- (26) Gavezzotti, A. *New J. Chem.* **2011**, 35, 1360–1368. The computer program package is available for distribution at <http://users.unimi.it/gavezzot>, upon notification to the author.
- (27) Frisch, M. J.; et al. *Gaussian 03*; Gaussian Inc.: Wallingford, CT, 2004.
- (28) Williams, D. E. *Acta Crystallogr.* **1971**, A27, 452–455.

- (29) van Eijck, B. P.; Kroon, J. *J. Phys. Chem.* **1997**, *B101*, 1096–1100.
- (30) Civalleri, B.; Maschio, L.; Ugliengo, P.; Gavezzotti, A. *J. Phys. Chem. B* **2011**, *A115*, 11179–11186.
- (31) Stievano, L.; Tielens, F.; Lopes, I.; Follier, N.; Gervais, C.; Costa, D.; Lambert, J.-F. *Cryst. Growth Des.* **2010**, *10*, 3657–3667.
- (32) Dalhus, B.; Görbitz, C. H. *J. Mol. Struct. (Theochem)* **2004**, *675*, 47–52.
- (33) Grimme, S. *J. Comput. Chem.* **2006**, *27*, 1787–1799. Moellmann, J.; Grimme, S. *Phys. Chem. Chem. Phys.* **2010**, *12*, 8500–8504.
- (34) van de Streek, J.; Neumann, M. A. *Acta Crystallogr.* **2010**, *B66*, 544–558.
- (35) Sun, C. C. *J. Pharm. Sci.* **2007**, *96*, 1043–1052.
- (36) Dovesi, R.; Saunders, V. R.; Roetti, C.; Orlando, R.; Zicovich-Wilson, C. M.; Pascale, F.; Civalleri, B.; Doll, K.; Harrison, N. M.; Bush, I. J.; D'Arco, P.; Llunell, M.; Università di Torino, 2009.